Photoluminescence of excitons bound to an isoelectronic trap in silicon associated with boron and iron

H. D. Mohring, J. Weber, and R. Sauer
Physikalisches Institut (Teil 4) der Universität Stuttgart, Pfaffenwaldring 57, D-7000 Stuttgart 80, Federal Republic of Germany
(Received 1 November 1983)

We describe the luminescent properties of an isoelectronic trap in silicon which needs boron and iron for its formation. The radiative recombination is due to an exciton localized at the trap. It exhibits no-phonon lines at 1.066 40 and 1.066 76 eV corresponding to dipole-forbidden and dipole-allowed transitions from $J=2$ or $J=1$ exciton states split by 0.36 meV due to the electrostatic electron-hole interaction. The exciton couples strongly to a quasilocalized mode of 9.7-meV quantum energy, resulting in one- and two-phonon Stokes replicas of the no-phonon luminescence spectrum. The rather large oscillator strength of the "forbidden" transition in the local-mode spectrum indicates that the optical center is a hole trap. We discuss the formation and dissociation of the trap and show that essential luminescence data are inconsistent with an identification of the optical center with Fe_iB_s pairs.

I. INTRODUCTION

Radiative recombination of excitons bound to isoelectronic impurities was originally discovered in several II-VI and III-V compound semiconductors in the early 1960s and since then has been intensely studied.[1] Such impurities were either single-point defects such as N or Bi in GaP substituting for a host atom on a lattice site[2,3] or "molecularlike" traps of noncubic symmetry such as ZnO or CdO pairs in GaP (Refs. 4 and 5) including even more complex aggregations as, e.g., the Li-Li-O trap in GaP.[6] Contrary to this situation, luminescence due to isoelectronic traps was not observed in silicon until 1979, when Weber *et al.*[7] detected an optically active axial isoelectronic defect, but could not identify its chemical nature. In the few years since this time, several more examples of luminescing isoelectronic traps in silicon have been reported and partially positively identified. Today, there are five other optical centers, in addition to the A,B,C trap of Weber *et al.*, which give rise to long-lived photoluminescence (PL) lines, and are therefore often labeled "isoelectronic" although only some of them exhibit the characteristic level scheme related with classical isoelectronic excitons: (1) The P,Q,R photoluminescence line system was originally detected by Vouk and Lightowlers[8] and then studied by Mitchard *et al.*[9] and other groups.[10,11] This spectrum can be created at large intensities in quenched In-doped silicon crystals. It was recently ascribed to an axial defect along ⟨001⟩ incorporating Fe and In.[12] The importance of Fe in the formation of the defect was first corroborated by Schlesinger and McGill,[13] but Schlesinger *et al.*,[14] in subsequent work from the absence of an observable Fe isotope shift, cast considerable doubt on the Fe-based model. (2) Two interdepending sets of photoluminescence lines were observed in quenched Tl-doped silicon by Thewalt *et al.*,[15] who suggested that they are due to two different configurations of an isoelectronic defect incorporating Tl. Schlesinger and McGill[13] found that Fe is also important in the formation of this defect, whose low-temperature configuration has obviously trigonal symmetry.[12] (3) Weber *et al.*[16] and Watkins *et al.*[17] recently reported on an isoelectronic center in quenched Cu-doped silicon, and the former group argued that a Cu pair in a ⟨111⟩ configuration is involved in the optical center. (4) An entirely different isoelectronic defect is responsible for the long-lived multiple J lines at 1.108 eV, which show up after irradiation damage of silicon and subsequent thermal or laser annealing.[18] This spectrum is due to a trigonal center[12] of unknown origin. (5) Finally, the investigations of Henry *et al.*,[19] Killoran *et al.*,[20] and Thewalt *et al.*[21] demonstrated that Be pairs in silicon can form an isoelectronic, ⟨001⟩ axially symmetric defect giving rise to the observed extraordinarily strong luminescence. The Be pair appears to be the only example of an isoelectronic defect in silicon whose chemical nature has positively been identified.

In this paper, we describe a new photoluminescence spectrum which reveals properties similar to classical pointlike isoelectronic traps. Nevertheless, the optical center is believed to be not a single impurity but a molecularlike aggregation as it forms in boron-doped silicon which is Fe diffused or doped with Fe in the melt. We subdivide this paper into several sections. First, we describe and discuss the optical spectra characterizing the binding center in terms of an isoelectronic hole trap. Then we discuss the formation and dissociation conditions of the center. A comparison with results from other analytical methods shows that essential luminescence data are contradictory to an identification of the optical center with Fe_iB_s pairs which are well studied in literature. Part of the present experimental material has been very briefly communicated elsewhere.[12]

As in former works,[7,16] we used a standard optical setup for the experiments. The samples were either immersed in boiling or pumped liquid helium or cooled by a helium-gas stream in a temperature-controlled Dewar.

The luminescence was excited by an Ar^+ laser (514 nm, ≤ 1.5 W) or a Kr^+ laser (647 nm, ≤ 600 mW). A monochromator of 1-m focal length equipped with ruled gratings (1200 or 600 grooves/mm) dispersed the luminescence signals which were then detected by a cooled Ge detector (North Coast) and processed by conventional lock-in–amplifier technique. Zeeman measurements were performed in a superconducting cryomagnet with a split-coil configuration. The sample preparation technique is described in detail in Sec. V.

II. BASIC PHOTOLUMINESCENCE SPECTRA

The new spectrum which we observe (Fig. 1) extends from ≈ 1.16 μm to wavelengths longer than 1.30 μm. It is composed of different contributions. On the high-energy side, two narrow lines $FeB^0_{0,1}$ (denoting the combined unresolved lines FeB^0_0 and FeB^0_1 in Fig. 2) and FeB^0_2 appear, which we identify as no-phonon (NP) radiative transitions of the exciton, bound to the center, believed to incorporate at least Fe and B. In our notation, subscripts denote electronic ground (0) or excited (1,2,...) states of the localized exciton, and upper indices denote NP transitions (0) or local mode satellites (1,2,...) where positive numbers refer to Stokes satellites and negative numbers to anti-Stokes satellites. The NP luminescence in Fig. 1 is replicated twice at displacement energies of 9.7 and (9.7 + 9.1) meV, giving rise to the pairs of quasilocal-mode sidebands $FeB^1_{0,1}$, FeB^1_2 and $FeB^2_{0,1}$, FeB^2_2, respectively. The origin of the succeeding relatively narrow triple structure at ≈ 1.195 μm and of the three distinct bands between the triple structure and $FeB^0_{0,1}$(TO) is unclear. We identify the line $FeB^0_{0,1}$(TO) as a replica of the $FeB^0_{0,1}$ line spectrum due to the coupling of a momentum-conserving optical phonon, and part of the following irregular structure may reflect the local-mode spectrum in the TO regime. All narrow line structure is superimposed on a broad band forming a smooth background. The background consists of both single and multiple acoustic-phonon replicas and acoustic- plus TO-phonon replicas. We conclude this from the temperature evaluation of the spectrum leaving behind, at $T > 60$ K, two corresponding broad bands displaced from each other by ≈ 58 meV, the relevant TO-phonon energy. The line positions and other data are listed in Table I.

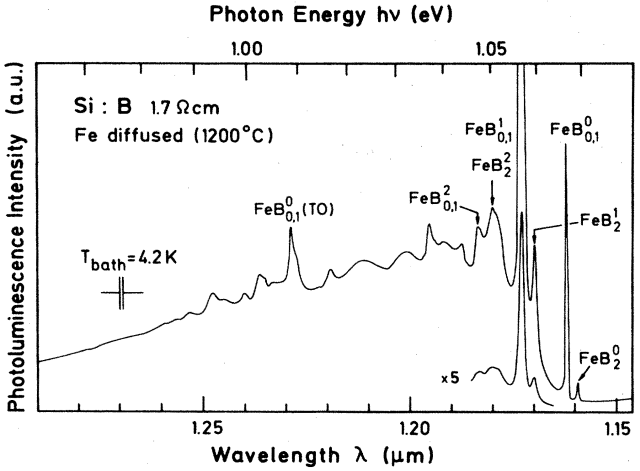

FIG. 1. Photoluminescence spectrum (intensity in arbitrary units) observed in boron-doped, iron-diffused crystalline silicon. Notation of lines: Upper index denotes number of local modes emitted in the event of the optical transition. Subscripts refer to electronic ground and excited states of the exciton giving rise to the luminescence. Excitation of the spectrum with Ar^+ laser, 514 nm, at a level of ≈ 500 mW. Spectral resolution is $\Delta\lambda = 0.6$ nm.

Figure 2 shows the high-energy portion of the spectrum in detail. The NP luminescence is weak at low temperature, $T = 1.6$ K, exhibiting the line FeB^0_1 and the much less intense FeB^0_0. The latter line, although only scarcely above the noise level, is reproduced at this low temperature. Under the perturbation of a magnetic field (see Sec. IV) this weak transition exhibits increasing total intensity quadratically depending on the field strength. The third NP line, FeB^0_2, is much broader than its NP companions and arises at elevated temperatures. This threefold NP line spectrum is replicated at 9.7 meV lower energies with two major differences. First, the line replicas are broader than the NP lines, and second, the "forbidden" FeB_0 transition is predominant at low temperatures. In this local-mode spectrum, we cannot completely resolve lines FeB^1_0 and FeB^1_1; however, it is clearly seen that the maximum intensity is shifted from FeB^1_0 at low temperatures to FeB^1_1 at higher temperatures, suggesting that the intensity ratio follows a Boltzmann factor. Eventually, the transition la-

TABLE I. Line positions and half widths of photoluminescence and photoluminescence excitation (PLE) spectra at 4.2 K unless otherwise specified. (PLE data courtesy of J. Wagner.)

Notation	Photon energy (eV)	Linewidth (meV)	Remarks
	Photoluminescence data		
FeB^0_2	1.0692_5	0.3[a]	No-phonon
FeB^0_1	1.0667_6	0.14	spectrum
FeB^0_0	1.0664_0		
FeB^1_2	1.0595	1.1	Stokes,
FeB^1_1	1.0570_3	0.6[b]	one local
FeB^1_0	1.0566_7	0.6[c]	phonon, $\hbar\omega = 9.7$ meV
FeB^2_2	1.0504	3	Stokes,
$FeB^2_{0,1}$	1.0476		two local phonons
$FeB^0_{0,1}$(TO)	1.0089	1.2	TO momentum conserving
	Photoluminescence excitation data		
FeB^0_2	1.0692	0.5	No-phonon spectrum
$FeB^{-1}_{0,1}$	1.0772		Anti-Stokes,
FeB^{-1}_2	1.0805		excited
$FeB^{-2}_{0,1,2}$	1.0860		upper state

[a]Measured at 6 K.
[b]Estimated at 4.2 K.
[c]Estimated at 1.6 K.

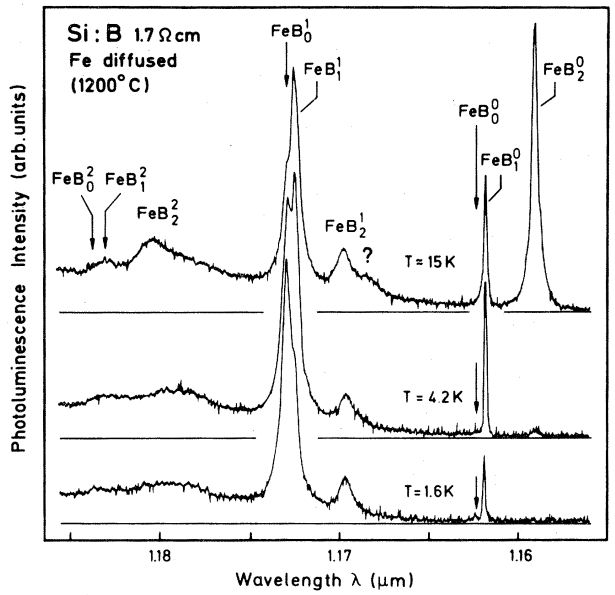

FIG. 2. High-energy portion of the spectrum exhibiting the no-phonon (NP) and the one- and two-phonon Stokes spectra. Spectral resolution is $\Delta\lambda=0.1$ nm. For line positions, see Table I.

beled FeB_2^1 could be the phonon replica of the FeB_2^0 line judged from the correct 9.7-meV energy shift. The FeB_2^1 line increases relative to $FeB_{0,1}^1$ when the temperature is raised, but not to the degree which is exhibited in the NP spectrum. In addition, the relatively strong observation of this transition at 1.6 K casts some doubts on this possible identification as the excited luminescent state should in practice be entirely depopulated. The line ? in Fig. 2, on the other hand, cannot be the phonon replica of FeB_2^0 based on energetic arguments. However, this line could be a second phonon replica of FeB_0^0 of a different quantum energy, but there is no further evidence for this assumption. So the true origin of the lines ? and FeB_2^1 remains unknown. A second replica of the whole NP spectrum, viz., the lines FeB_0^2, FeB_1^2, and FeB_2^2, is generated by the coupling of two quanta of the 9.7-meV vibration mode to the optical transition. Since these lines are in turn broader than the lines of the first replica and of the NP spectrum, they appear, at weak intensities, in the well-resolved spectrum in Fig. 2. For the "allowed" transition, FeB_1, we estimate that the integrated intensity of the NP line to the intensities of the one-phonon and the two-phonon lines is approximately 1:7:0.5 at 4.2 K. The corresponding total intensities of the FeB_1^0 line and the broad continuum band are in an estimated ratio of 1:75.

The properties of the luminescence spectrum previously described are, in principle, similar to several other luminescence systems and characterize the exciton as an electron-hole pair which is localized at an isoelectronic trap. *J-J* coupling of the electron and the hole forms two energetically close exciton states spaced by 0.36 meV due to the electrostatic interaction of the two particles. The higher-energy state, which we label $J=1$, decays radiatively to the crystal ground state, $J=0$, via a dipole-allowed transition. Dipole transitions are not allowed from the lower-energy state labeled $J=2$. The large oscillator strength gained by the "forbidden" transition FeB_0 in the local-mode spectrum is an important fact. Similar behavior in the classical case of GaP:Bi led Hopfield *et al.*[22] to distinguish between isoelectronic donors and acceptors. They argued that the primary particle, when it is tightly bound to the short-range potential of the trap, is mainly responsible for the phonon coupling. When the trap is an isoelectronic donor it captures first a hole (Γ_4 symmetric in GaP) which can cause strong coupling to phonons of symmetry Γ_1, Γ_3, and Γ_4, and cross-couple between the $J=2$ and $J=1$ exciton states when the spin-orbit coupling is accounted for. As a result, the total optical decay rates from the $J=2$ or 1 exciton states will be comparable at equal populations of the states, whereas the relative NP strength of the $J=2\rightarrow 0$ transition will be weak compared to its one-phonon sideband. Experimentally, we encounter exactly this situation in our spectra. Theoretically, the symmetry of holes from the Γ_8 valence-band edge is Γ_5^+ in silicon, neglecting spin-orbit interaction, and will lower to Γ_5 when the hole is localized at the trap. The operator describing the phonon coupling transforms as $\Gamma_5\times\Gamma_5=\Gamma_1+\Gamma_3+\Gamma_4+\Gamma_5$, where Γ_4 is disregarded as only the symmetric part of the product group gives the symmetry of the phonons. Therefore, only vibration modes of $\Gamma_1(A)$, $\Gamma_3(E)$, or $\Gamma_5(T_2)$ symmetry couple to the trapped hole. The $J=2$ and 1 exciton states are cross-coupled by the E and T_2 modes via the spin-orbit coupling but not by the A modes, and the different oscillator strengths in the NP spectrum and the phonon replica are due to E or T_2 modes. We note this result for further discussion in Sec. VI.

Photoluminescence excitation (PLE) spectroscopy has also been successfully applied to the present trap. This experiment was performed by J. Wagner, who kindly contributed the PLE spectrum (Fig. 3). The color-center laser operating with NaF:Ca(F_2^+)* as the active medium and tandem pumped by a 1,1',3,3'-hexamethylindotricarbocyanine perchlorate (HITC) dye laser and a Kr^+

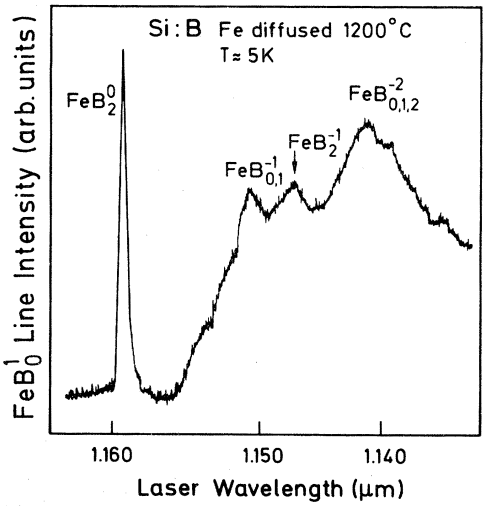

FIG. 3. Photoluminescence excitation spectrum reflecting vibronic structure of excited, upper trap state (courtesy of J. Wagner). For line positions, see Table I.

laser was described elsewhere.[23,24] It could be tuned over the wavelength range 1.01 to 1.16 μm. The output power in the range 1.13 to 1.16 μm was 30 mW. The enlarged spectral range is due to the modified spectral characteristics of the output mirror. The PLE spectrum was obtained by recording the one-phonon Stokes $FeB^1_{0,1}$ luminescence transition while the laser was tuned. The PLE spectrum continues the PL spectrum that exhibits, on the low-energy side, the FeB^0_2 line which we already observed in photoluminescence. Three other features are observed at higher energies which we clearly identify as one- and two-phonon anti-Stokes transitions due to the coupling of a 10.8-meV vibrational mode to the excited upper trap state and similar in size to the 9.7-meV mode of the defect ground state. The energetic positions of the lines are listed in Table I. No further excited state could be detected up to the band edge at ≈ 1.060 μm.

The PL and PLE data reported so far give evidence for the level scheme of the luminescent trap which is presented in Fig. 4, showing various electronic and vibronic states. The nature of the vibronic states has already been discussed. The magnetic labels used in the scheme are anticipated from Sec. IV. The ground state of the localized exciton is split by 0.36 meV due to the electrostatic interaction of the $J=2$ and 1 states. The magnetic labels are rather good quantum numbers, as the $J=2$ transition is relatively strictly forbidden different from other isoelectronic systems, as, e.g., the Cu-related trap in silicon[16] or the "classical" N trap in GaP.[2] The exciton ground-state transition at 1.0664 eV defines an exciton localization energy to the trap with respect to the low-temperature band edge at $E_g(4.2\ \text{K})=1.1695$ eV of $E_{BX}=103.1$ meV. The $J=2$ and 1 states exhaust the eightfold degeneracy of the localized exciton formed from a Γ_6 and a Γ_8 hole. Therefore, the 2.85-meV excited level cannot be due to the same orbital exciton state. The excitation energy is, on the other hand, so low that it is difficult to associate it with an orbitally excited state. A possible explanation could be to ascribe the level to an electron bound to the hole in a low-lying Jahn-Teller-like state. This state could result from the strong coupling of low-energy E and T_2 modes similar to the excited 4.2-meV Jahn-Teller state of the indium acceptor in silicon.[25,26] Sections III and IV will serve to support the level scheme in Fig. 4 by temperature-controlled measurements and Zeeman measurements.

III. TEMPERATURE DEPENDENCE

PL spectra were recorded from 1.6 up to 160 K and a few of them are plotted in Fig. 5. From about 10 K and higher, the NP spectrum is dominated by the excited-state line FeB^0_2. (Note, in comparison to Fig. 2, the different spectral resolution, overrepresenting, in Fig. 5, the broader lines.) The corresponding line FeB^1_2 in the one-phonon spectrum is relatively much weaker, but increases as well, clearly exhibiting that it is in (quasi)equilibrium with FeB^1_1 and FeB^1_0. In the two-phonon spectrum, Fig. 5 shows only the excited-state line FeB^2_2 which is predominant in this spectrum from about 8 K and higher. In comparing the total intensities in the various phonon replicas, the NP spectrum grows relatively much more rapidly than the phonon-assisted spectra, and is the strongest spectrum up to 60 K, where all sharp line structure has essentially vanished. The two-phonon spectrum increases over the entire temperature interval (1.6 to 60 K) in relation to the one-phonon spectrum. From about 70 K and higher, the spectrum chiefly exhibits the broad band which is due to the coupling of the low-frequency, acoustic-mode continuum and which appears as a sideband to the NP spectrum as well as to the TO-phonon—assisted spectrum. The TO-phonon—related band grows further, relative to the NP-related band, and is the strongest feature from about 160 K and higher.

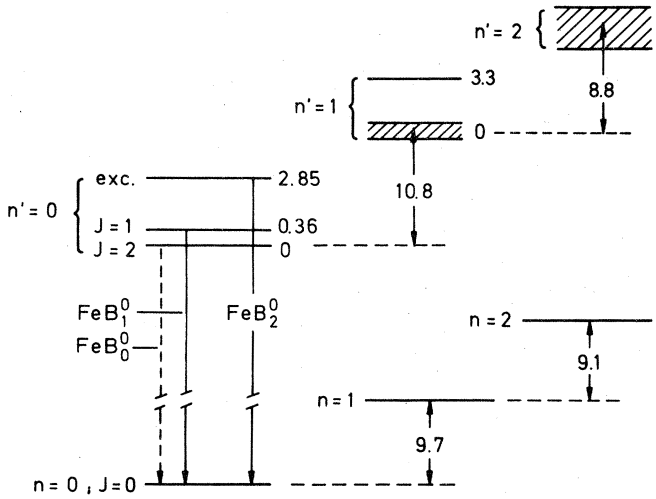

FIG. 4. Level scheme of the optical center. Labels n and n' denote vibronic quantum numbers of defect ground state or transition upper excited defect state, respectively. Energies are given in meV. For clarity, from all observed transitions only three NP transitions are drawn.

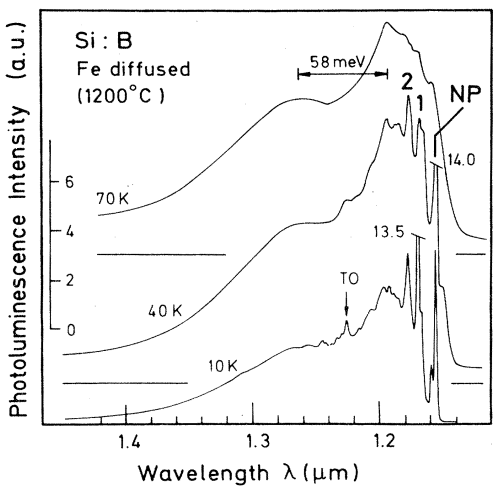

FIG. 5. Photoluminescence spectra (intensity in arbitrary units) at three higher temperatures. Spectral resolution is $\Delta\lambda=1$ nm. Labeled are the NP, the one-phonon (1), and the two-phonon (2) spectra. Numbers at cutoff lines indicate line intensities in units of the left-hand scale.

The maxima of the two bands are spaced by ≈ 58 meV, equal to the energy of the momentum-conserving TO phonon at $\vec{k}=0.85(\pi/a)(1,0,0)$, the location of the conduction-band minimum in the Brillouin zone. The fact that the NP spectrum and its acoustic-mode band is clearly observed as a TO replica leads us to suppose that the sharp line features seen at low temperatures energetically below 1.23 μm are local-mode satellites of the $FeB^0_{0,1}$(TO) transition. The identification of these lines is not yet quite clear.

To check our suggestion that the population of the exciton states decaying via lines FeB^0_2 and FeB^0_1 are in thermal equilibrium, in Fig. 6 we plot the ratio of the PL intensities as a function of temperature. The fit in Fig. 6 is an Arrhenius plot with a thermal activation energy of 2.4 meV. This value is equal to the spectroscopic spacing, 2.49 meV, of the lines FeB^0_2 and FeB^0_1 within experimental uncertainty of the temperature-controlled experiment.

The absolute intensities of the lines FeB^0_2 and FeB^0_1 as a function of temperature are depicted in Fig. 7. Line FeB^0_2 is activated with an energy of ≈ 3 meV and grows up to about 20 K, from which it is rapidly quenched with a deactivation energy of ≈ 25 meV. Line FeB^0_1 reveals a moderate initial increase from 1.6 to 4.2 K which is not shown in Fig. 7 and is consistent with the spectroscopic spacing of 0.36 meV between the lines FeB^0_0 and FeB^0_1. After a maximum extending from ≈ 5 to ≈ 10 K, line FeB^0_1 is also rapidly quenched.

In the following, we discuss the question of whether the observed deactivation is due to the dissociation of the localized exciton or to the vibronic coupling. To consider the dissociation first, we performed a fit to the experimental points of FeB^0_2 by using the analytical expression

$$I(T)=I(0)[1+C_1\exp(-E_1/kT)+C_2\exp(-E_2/kT)]^{-1},$$

which represents the solid line in Fig. 7, with the set of parameters $E_1=-3.1$ meV, $C_1=0.078$, and $E_2=25.5$ meV, $C_2=1.28\times 10^5$. This expression has physical meaning if it is assumed that the excited excitons are partitioned between electronic states with no vibronic coupling. Then the factors C_i stand for the ratios $C_i=g_i\tau_0/g_0\tau_i$

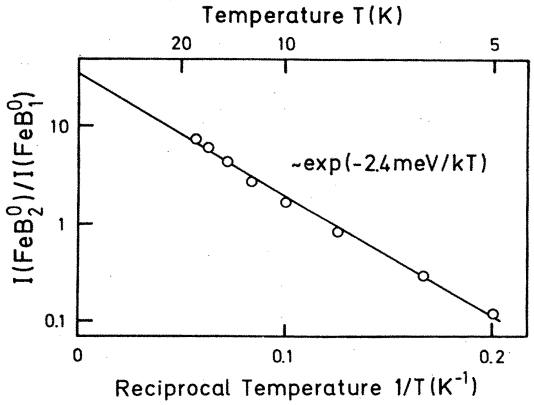

FIG. 6. Intensity ratio of the line FeB^0_2 to the line FeB^0_1 as a function of temperature. Circles are experimental, and the solid line represents a least-squares Arrhenius fit to the circles, giving a thermal activation energy of 2.4 meV.

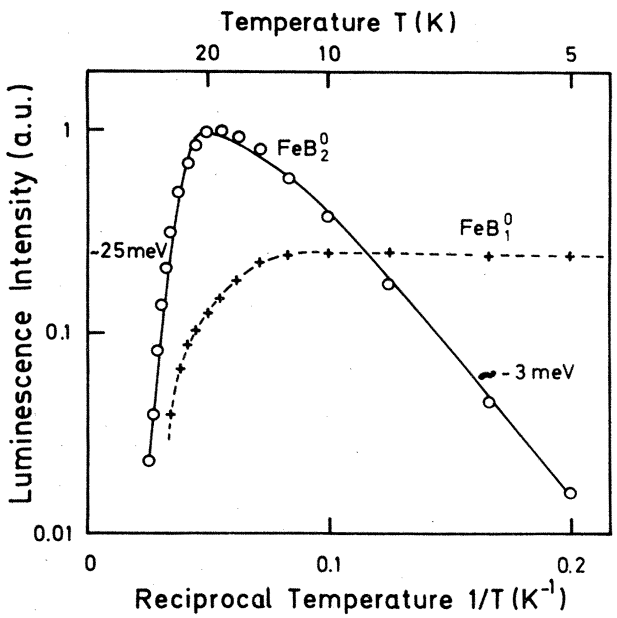

FIG. 7. Absolute intensities (in arbitrary units) of lines FeB^0_1 and FeB^0_2 as a function of temperature. Circles and pluses are experimental. The dashed line is an optical guide, and the solid line represents a least-squares fit; see text.

where g_0 and g_i are the degeneracies of the exciton ground and excited states and τ_0 and τ_i are the corresponding lifetimes of these states. The formula for $I(T)$ implies that under stationary conditions the excitons are generated at a rate equal to the sum of all recombination rates. If we neglect vibronic coupling for the moment, we may conclude from the very large factor C_2 that this term describes the dissociation of the exciton complex into a band. The 25-meV dissociation energy is much less than the spectroscopic binding energy, $E_{BX}=103.1$ meV, and suggests that only one particle is thermally released from the complex. We assume that the electron is lifted to the conduction band since it was shown that the defect is an isoelectronic donor. Remaining with this model, we may then improve the expression for $I(T)$ by replacing C_2 by $C_2'T^{3/2}$, taking into account the density of states in the band continuum. As a result, we find a lower deactivation energy of FeB^0_2, $E_2=17$ meV. This value when combined with $E_{BX}=103.1$ meV would characterize a position of the donor trap in the forbidden gap, E_v+86 meV. This is very close to the value of E_v+88 meV which was preliminarily communicated by two of the authors.[12]

Actually, from the low-temperature spectra in Figs. 1 and 2, where the one-phonon sideband is much more intense than the NP spectrum, vibronic coupling seems to be significant. However, even at temperatures well below 20 K before the quenching of the NP spectrum is initiated, the NP lines dominate all other discrete line features (compare also the 40-K spectrum in Fig. 5) and tend to become even more paramount upon further temperature increase. Therefore, it is rather questionable whether the coupling of the discrete local modes to the optical transition causes an appreciable contribution to the FeB^0_2 line quenching from 20 K and higher. On the other hand, the coupling to the acoustic-mode continuum has to be re-

garded since the continuum band monotonically increases (Fig. 5) and eventually dominates from about 70 K and higher. We estimate the importance of the band for the temperature dependence of the NP lines closely following along the lines given by Gislason *et al.*[27] in their discussion of the Cu-related 2.177-eV col spectrum in GaP. In this approach, we shall completely neglect the discrete phonon sidebands for the reasons mentioned above. As was noted earlier, the low-temperature integrated intensities of the NP spectrum to the acoustic-mode band are approximately 1:75. This gives a Huang-Rhys factor of $S_{\text{band}} \approx 4.3$. The total Franck-Condon shift of the band corresponds to the maximum of the band which at high resolution is located close to 1.20 μm so that a Franck-Condon shift of ≈ 35 meV results with respect to the position of the FeB_1^0 line. These values, 35 meV and $S=4.3$, yield ≈ 8 meV as an average phonon energy. This is in the linear portion of the acoustic-mode dispersion curves and allows us to approximately describe the low-frequency continuum modes of the crystal with the Debye approximation. Thus we have[27]

$$S(T)=S[1+\tfrac{2}{3}\pi^2(T/\Theta)^2] ,$$

where $\Theta=645$ K is the Debye temperature of silicon as obtained from specific-heat measurements. The expression for the NP intensities,

$$I(T) \propto \exp[-S(T)] ,$$

represents a horizontal line from low temperatures to above 40 K. For example, at 80 K we have $I(T)/I(0)=0.85$, and even much lower values of Θ cannot explain the observed intensity decrease in Fig. 7 in the assumed model.

As a result of these considerations, we find a pronounced discrepancy. At a temperature of 40 K, for instance, the exciton should be entirely dissociated if the ionization energy is 17 meV since the density of states in the band is very much higher than for the exciton. It is difficult to understand why the phonon band is so strong, which in the model discussed is generated by the coupling to the exciton transition. To evade the discrepancy it seems reasonable to assume that the vibronic coupling is relatively weak in the exciton ground state but is appreciably stronger in the 2.85-meV electronic excited state. The associated line, FeB_2^0, increases by a factor of ≈ 100 up to 20 K, and a large coupling strength could explain the dramatic increase of the phonon band as well as the observed fast deactivation of the NP line for higher temperatures. This interpretation implies that we cannot determine one-particle binding energies from our temperature-dependent PL data.

IV. ZEEMAN MEASUREMENTS

We studied the NP lines FeB_0^0 and FeB_1^0 in magnetic fields up to 5.3 T. The magnetic field perturbation makes transitions from the $J=2$ exciton manifold allowed, and we observe them from ≈ 1 T and greater. Spectra were recorded in transverse observation (Voigt configuration) with the field aligned along the crystal directions ⟨001⟩, ⟨111⟩, and ⟨110⟩. For these directions, the two lines

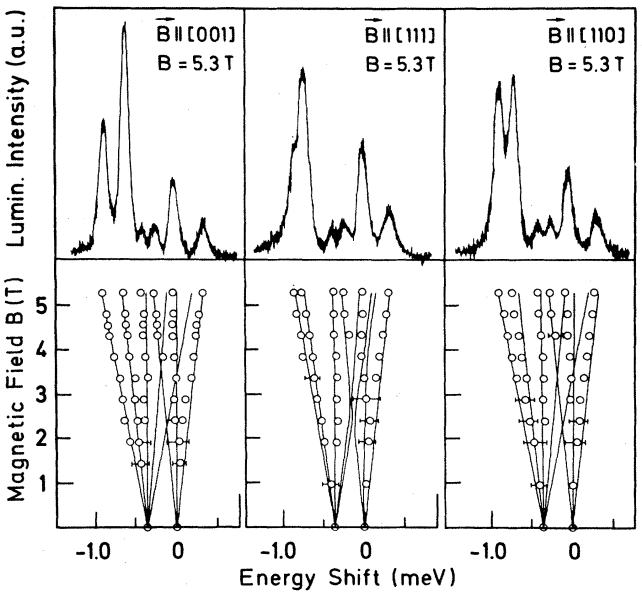

FIG. 8. Zeeman splitting of lines FeB_0^0 and FeB_1^0. Intensities of spectra in arbitrary units (upper part). The zero of energy refers to the position of line FeB_1^0. The Zeeman components are essentially unpolarized. Open circles in the lower part are experimental, and bars indicate broadening of lines. Solid lines represent a fit using the most general Zeeman Hamiltonian in T_d for a coupled electron-hole pair (see text).

split each threefold (Fig. 8). The two inner, weak components can only be resolved at the higher fields, but from the field dependence it is probable that the three left-hand lines belong to FeB_0^0 and the three right-hand lines to FeB_1^0. The two high-lying components clearly thermalize. The ratio of the intensities of the two strong low-lying components varies only weakly when the line spacing increases with the applied field, inconsistent with a full thermalization. The Zeeman patterns are similar for the three field directions: the major difference being the anisotropy in the positions of the two low-lying components. The dependence of the spectra at 5.3 T on the orientation of the field with respect to the crystal axes is plotted in Fig. 9. Except for the two low-energy lines, all other Zeeman components shift only very slightly in energy.

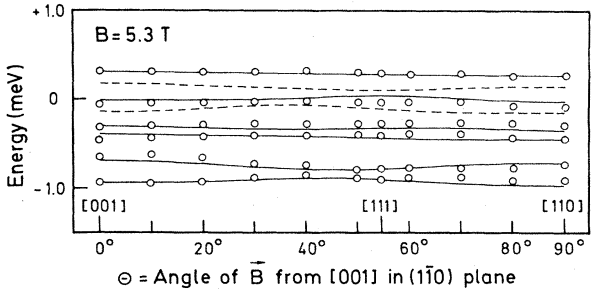

FIG. 9. Orientational dependence of Zeeman spectra. Open circles are experimental, and solid lines represent fit as in Fig. 8. Dashed lines refer to the transitions from the exciton states $|J,M_J\rangle = |2,2\rangle$ and $|2,1\rangle$ which thermalize with the lower states of the $J=2$ manifold (cf. Fig. 8) and are not experimentally observed.

Important in the discussion of the data are the observations that both exciton states previously labeled $J=2$ and 1 are at least threefold degenerate and that no crossings occur in the orientational dependence as would be typical for states characterized by an axis. This forbids classification of the exciton ground state as $J_z=\pm 2$ and ± 1 according to the model discussed by Morgan and Morgan,[28] although this choice would be suggestive with regard to the 2.85-meV excited level which could then be ascribed to the states $|J,M_J\rangle=|2,0\rangle$, $|1,\pm 1\rangle$, and $|1,\pm 0\rangle$. Since any site symmetry lower than cubic gives rise to a preferential axis, provided the symmetry affects the magnetic coupling, we are confined to T_d symmetry with an interpretation. This is at variance with the anticipated axial nature of the defect.

We performed tentative fits using the secular matrix of Merz *et al.*[29] This applies to Γ_3, $\Gamma_4(J=2)$, and $\Gamma_5(J=1)$ exciton states formed from the coupling of a Γ_6 electron with a Γ_8 hole in T_d and corresponds to the most general linear Zeeman interaction. The fit in Figs. 8 and 9 results when we neglect a cubic field splitting between the Γ_3 and Γ_4 exciton states while the $\Gamma_{3,4}$-Γ_5 splitting is taken to be 0.36 meV, and when we choose the parameters

$$\gamma_1=1.0,\ \gamma_2=0.9,\ \gamma_3=0.9,\ \delta_1=0.2,\ \delta_2=0.1\ .$$

This set fits the experimental points satisfactorily and is not too inconsistent with the relations among the γ_i and δ_i which were derived by Merz *et al.* from group theory:

$$\delta_1=\tfrac{1}{2}(\gamma_1-\gamma_2)\ \text{ and }\ \delta_2=\tfrac{1}{2}(\gamma_1+\gamma_2)-\gamma_3\ .$$

This model, however, is not consistent with a particular thermalization feature. It predicts that the inner Zeeman component originating in the excited $|1,-1\rangle$ exciton state (Fig. 8) should be much stronger than it is experimentally since this state thermalizes with the $|1,0\rangle$ and $|1,+1\rangle$ states emitting the two high-lying Zeeman components.

We also tried to apply another model by assuming that a large cubic field splits the $J=2$ state into the threefold exciton ground state Γ_4 and an excited twofold Γ_3 state which we then identified as the 2.85-meV state, whereas the assignment of the Γ_5 state remained unmodified. Under these assumptions we did not find a fit which is in any way compatible with the empirical data. Experimentally, we cannot study the Zeeman splitting of the excited state in our cryomagnet and cannot, therefore, decide whether this state is twofold degenerate. Apart from this, a cubic field splitting of 2.85 meV seems exorbitantly high although there is no value for comparison in silicon. In GaP, crystal-field splittings of the $J=2$ state of excitons at isoelectronic traps were observed and are one order lower. For the Bi bound exciton, Dean and Faulkner[30] found a splitting of 0.28 meV, and Merz *et al.*[29] observed a splitting of 0.16 meV for the excitonic molecule bound to nitrogen.

The total intensity of all components from FeB_0^0 to the total intensity of all components from FeB_1^0 varies as the square of the field strength (Fig. 10). This is due to the linear admixture of wave functions from $J=1$ to those of $J=2$ in the interaction matrix, and is similarly observed for other isoelectronic excitons in silicon, e.g., for the

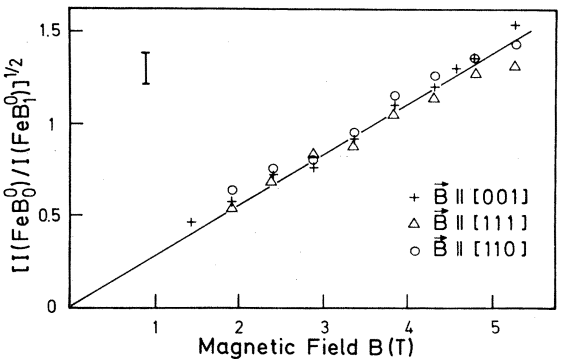

FIG. 10. Ratio of integrated intensities of the FeB_0^0 Zeeman components to the FeB_1^0 components versus field strength B. The estimated error of the experimental values is indicated by the bar. The solid line is an optical guide and corresponds to a square dependence on B.

A,B,C-line system[7] or the exciton bound to Be pairs.[19]

To conclude this section, it is not clear how significant the fits are which we attempted. In particular, the values of γ_i and δ_i communicated above lead to g factors[29] $g_e=0.75$, $K=0.95$ and $L=0$, where K and L characterize the isotropic or anisotropic splitting, respectively, of the hole. We have argued that we are concerned with an isoelectronic donor and would therefore rather expect a g value of the more loosely bound electron close to 2. Also, there is the problem with the relative Zeeman intensities on the specific model. These points cast some doubts on the simple interpretation of the Zeeman data in T_d symmetry although alternative approaches are not obvious.

V. SAMPLE PREPARATION

This and the following section are devoted to the description of experiments related to the formation and dissociation of the luminescent defect aiming to identify its chemical nature. We observed the spectrum exclusively in boron-doped silicon but under various preparation conditions. The samples were either iron doped in the melt or iron diffused. However, not all samples exhibiting the luminescence were intentionally doped. The starting material for the diffused samples was dislocation free, floating-zone (FZ) silicon doped with boron in the concentration range 10^{13} to 10^{16} cm^{-3}. Sections of ≈ 400 μm thickness and edge lengths of 5—8 mm were cut, cleaned in acetone, and etched in a mixture of HF and HNO_3 (1:4) and a small amount of acetic acid. Iron was then brought up to the samples by evaporation in high vacuum or by rubbing a high-purity (99.999%) iron wire on the surfaces. The iron wire was etched in HCl immediately before rubbing. The diffusion of iron into the sample was performed in a quartz tube under a buffer-gas atmosphere of streaming argon, nitrogen, or oxygen. The quartz tube was installed in a vertical furnace from which the samples could be dropped into a liquid. Water tended to tear the samples, particularly when their size was larger, since the quenching rate is high and leads to strong internal tensions. Silicon oil is nondestructive but seems to produce only a moderately high quenching rate. We found as the

most appropriate liquid a mixture of ethylene glycol (thermal conductivity 0.25 $Wm^{-1}K^{-1}$) and water (0.7 $Wm^{-1}K^{-1}$) in the ratio 1:1 which exhibits a high quenching rate but does not destroy the samples. A quenching rate as high as possible is important because it generates high intensities of the PL spectrum under discussion possibly by preventing precipitation of iron. After the quenching, the remainder of the iron was removed by lapping with a finely grained abrasive (Mikrogrit, 1 μm). Subsequent, renewed etching yielded smooth, reflecting surfaces. The samples were then stored in liquid nitrogen.

VI. FORMATION AND DISSOCIATION OF THE TRAP

Samples prepared in this way at a diffusion temperature of 1200°C under Ar buffer gas show luminescence line groups at 1.7, 1.22, and 1.16 μm at different intensities. The first group is seen in high-resistivity material and vanishes for higher boron concentrations. It was first described by Weber and Wagner[31] to appear strongly in iron-diffused n-type material independent of the donor species. The line group at 1.22 μm was also seen by these authors. It was recently studied in detail by Weber *et al.*,[16] who demonstrated that the line group is due to a copper-related defect, and it was also ascribed to copper in a later study by Watkins *et al.*[17] As copper is a fast diffusor in silicon with a high solid solubility ($\approx 10^{18}$ cm^{-3} at 1200°C), it is a feared contaminator, and we are not surprised that this spectrum arises at moderate intensities in samples of higher resistivity. Originally, this spectrum was even detected in silicon unintentionally contaminated with Cu by Minaev *et al.*,[32] and could therefore not then be identified, but it was ascribed to a "thermally induced defect." This spectrum is largely suppressed in our present experiments when the boron doping level is higher. Simultaneously, the line group at 1.16 μm which was discussed in the preceding sections comes up generally and dominates all other spectral features.

Experiments under Ar or N_2 buffer gas are characteristically different from those under O_2 buffer gas. When we investigate control samples which we subjected to all cleaning procedures, but without bringing iron intentionally up onto the surface, we observe, after heating in Ar or N_2 atmosphere and quenching, the 1.16-μm luminescence at comparable intensities as in samples on which iron was deposited. This is not so with O_2 atmosphere where the control samples exhibit only extremely weak 1.16-μm luminescence but strong near-band-edge radiation. This discrepancy is similar to EPR measurements on a different, iron-correlated defect in silicon. Lee *et al.*[33] observed with EPR the incorporation of iron in an electrically active, thermally induced defect in silicon which was not intentionally doped with iron. They concluded that iron was contained in the sample before the heat treatment in the form of precipitates. Rijks *et al.*[34] demonstrated that the defect was not observed when the heat treatment was performed in a H_2 atmosphere together with a small amount of HCl gas and O_2. They argued that transition metals with large diffusion coefficients reach the samples as contaminations from external sources (e.g., the heater filaments of the furnace or from the quartz glass). Diffusion of the metal into the sample is prohibited, however, by the formation of volatile metal chlorides in conjunction with an oxygen layer on the sample surface. These data were corroborated by Weber and Riotte,[35] who observed iron diffusion from random sources into any silicon sample upon heat treatment. The iron contamination is prevented by a nonreducing atmosphere during the heating. Our samples doped with iron in the melt exhibit a similar behavior to the iron-diffused samples under O_2-gas atmosphere. They reveal the luminescence at 1.7 and 1.16 μm, whereas the Cu-related PL is absent. We conclude from these results that iron is needed to form the luminescent trap.

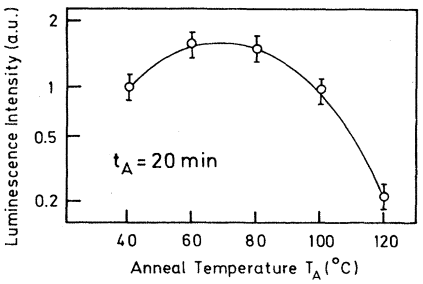

FIG. 11. Dependence of NP photoluminescence (intensities in arbitrary units) on isochronal annealing at an anneal time of 20 min.

Remaining with the O_2 buffer-gas atmosphere, we observe the following tendencies: When the boron doping concentration is enhanced the 1.16-μm PL increases. When we hold the boron concentration fixed at a higher level (e.g., 10^{16} cm^{-3}) and vary the diffusion temperature from 1000 to 1200°C the PL also increases strongly. The luminescence of excitons bound to boron acceptors is dominant at the lower temperature but disappears entirely at the higher temperature. We found it impossible to study the line intensities of the 1.16-μm PL quantitatively as a function of the diffusion temperature and the boron concentration as the intensities vary to a great extent even in identically treated samples cut from the same ingot. This is most probably due to the details of the quenching process where even small changes from one experiment to

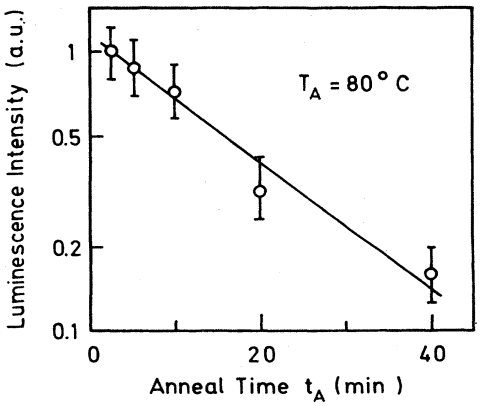

FIG. 12. Dependence of NP photoluminescence (intensities in arbitrary units) on isothermal annealing at an anneal temperature of 80°C.

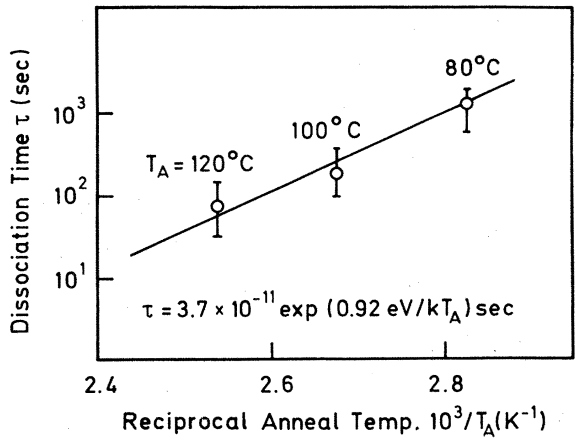

FIG. 13. Temperature dependence of dissociation time constant τ. The solid line is described by the expression on the bottom of the figure.

the next can cause large PL variations. One effect could, for instance, be the formation of vapor bubbles irregularly influencing the heat transfer to the liquid. Thus the tendencies which we have described are only qualitative, as obtained from many trials. They suggest that the optical center is associated with both boron and iron.

The annealing behavior of the trap was studied in samples exhibiting strong PL intensities. At an annealing temperature of $T_A = 60\,^{\circ}\mathrm{C}$, the 1.16-$\mu$m PL increases from a starting value directly after the quenching within a time interval of 20—40 min by a factor of ≈ 2 and then remains constant. At a fixed annealing time of $t_A = 20$ min, the PL intensities first increase upon an increase of T_A and then drop reaching a maximum between 60 and 80 °C (Fig. 11). The time dependence of the recovery for $T_A \geq 80\,^{\circ}\mathrm{C}$ was investigated at three temperatures and was found to be exponential, as specified for $T_A = 80\,^{\circ}\mathrm{C}$ in Fig. 12. The corresponding decay times are depicted in Fig. 13 and were fitted by an expression assuming the dissociation of the trap over an activation barrier U obtained from the fit as $U \approx 0.9$ eV. Finally, we probed the photodissociation of the trap. Two specimens were cleaved from a section of appropriately treated silicon and both were immersed in a water bath at various temperatures, but only one of them was illuminated by "white" light from an incandescent lamp. The luminescence of both specimens was then compared. At a bath temperature of 20 °C, no variation of the PL occurred after 15 h of illumination. At 40 °C, we observed an exponential photodissociation of the trap in the illuminated sample with a time constant of 1.8 h, whereas the twin sample exhibited no change in the PL intensity.

VII. DISCUSSION

Whereas the level scheme of the optical center is evident from the luminescence experiments, the nature of the center is not so easily identified. We conclude that the center needs boron for its formation since the 1.16-μm luminescence was never observed (apart from traces) in material not nominally doped with boron and is strongest for high boron concentrations. We may continue to conclude that boron is incorporated in the optical center although this reasoning is not necessarily true. There is the example of the Si-B3 defect as studied by Brower[36] with the EPR technique which obviously needs boron for its formation, but, nevertheless, boron could not be detected as a constituent of the EPR center investigated. Let us assume here that boron is incorporated in the luminescent trap. We have also given arguments suggesting that iron participates in the formation of the trap. This conclusion was essentially due to the diffusion experiments in O_2-gas atmosphere which could distinguish between intentional iron doping and uncontrolled iron contamination. By assuming once more that iron is *incorporated* in the trap it is suggestive to identify the trap as an iron-boron pair. This was recently done by two of the authors[12] on the basis of less experimental information than in the present more advanced study. In the following we shall discuss various aspects and show that important PL features conflict with the FeB pair interpretation.

It is well known that iron and boron form pairs in silicon. Iron diffuses interstitially in silicon with a high diffusion coefficient[37] ($D = 6 \times 10^{-6}$ cm^2/sec at 1200 °C) and high solid solubility[38] (10^{16} atoms/cm^3 at 1200 °C). Fast quenching (10^3 K sec^{-1}) after the diffusion freezes nearly all solved iron on interstitial sites of T_d symmetry.[35] Interstitial iron (Fe_i) forms a donor level at $E_v + 0.4$ eV.[33,39] Depending on the position of the Fermi level, the charge states Fe_i^+ or Fe_i^0 exist. While atomic iron possesses the outer electron configuration $3d^6 4s^2$, the $4s$ electrons pass over to $3d$ upon the interstitial incorporation into the silicon lattice and the configurations $3d^7(Fe_i^+)$ or $3d^8(Fe_i^0)$ result.[40] Interstitial iron is mobile at room temperature, and therefore, pair formation is possible in p-type silicon between a negatively charged substitutional acceptor and a positively charged Fe ion. Ludwig and Woodbury[41] studied pairs formed from iron and the shallow acceptors B, Al, Ga, and In by means of the EPR technique. All pairs except for Fe-In are ⟨111⟩ configurations. This direction characterizes an axis from a substitutional lattice site to a nearest interstitial site of T_d symmetry.

Energy levels due to single iron or iron-boron pairs have been reported by various authors.[39,41–46] Feichtinger[44] observed in Hall measurements that the iron level at $E_v + 0.4$ eV, as well as the boron acceptor level at $E_v + 0.045$ eV, disappear due to complexing. Instead, he observed the appearance of a donor level at $E_v + 0.1$ eV. This level was also reported by Graff and Pieper[45,46] from deep-level transient spectroscopy (DLTS) measurements. Eventually, Wünstel and Wagner,[47] in a recent work, also identified the level at $E_v + 0.1$ eV which they detected in Hall measurements and transient capacitance measurements with Fe_iB_s pairs.

In the present work, a collaboration with Wünstel and Wagner made it possible to investigate the same samples in photoluminescence and by DLTS measurements. About thirty samples exhibited the $E_v + 0.1$ eV FeB pair level *and* also showed the 1.16-μm luminescence lines. The signals in the two experiments were sometimes direct-

ly correlated, but there were also exceptions exhibiting the one signal but not the other. This finding may indicate that on one hand there is a narrow relationship between the EPR-Hall-DLTS centers and our PL center, e.g., in that they share common atomic constituents, but that on the other hand essential differences exist between the defects.

Sauer and Weber[12] reported a thermal dissociation energy of ≈ 15 meV of the exciton and compared the deduced primary particle binding energy to the PL trap of ≈ 88 meV with the DLTS level, $E_v + 100$ meV, of the FeB pairs. This comparison is no longer possible as we have shown that the deactivation of the main FeB_1^0 transition cannot be explained by the dissociation of the exciton but is essentially governed by the vibronic coupling.

In this paper, a thermal dissociation energy of the binding center of $U \approx 0.9$ eV (Fig. 13) was obtained. This is close to literature data for FeB pairs, viz., a dissociation energy of 1.17 eV (Feichtinger[44]) or 0.85 eV (Kimerling and Benton[48]). Likewise, our luminescent trap is photodissociated by white-light illumination as is the FeB pair.[45]

On the other hand, there are arguments contradicting the simple identification of the optical center with FeB pairs. Since boron is known to quantitatively pair with iron the FeB pair concentration amounts to the initial boron doping level. For definiteness, this may be assumed to be some 10^{14} cm^{-3} as, e.g., specified by Wünstel and Wagner.[47] Our PL intensities, provided they were associated with such trap concentrations, would have to be larger, by orders of magnitude, than we observe them. The 1.16-μm intensities are typically similar to the ones from boron bound excitons (BE's) when the boron concentration is of order 10^{14} cm^{-3}. The radiative quantum efficiency η of boron bound excitons is low because the dominant recombination mechanism is a localized Auger process giving rise to[49] $\eta = \tau_{\text{expt}}/\tau_{\text{rad}} = 2.16 \times 10^{-3}$. In the present case, we are concerned with an isoelectronic exciton and may, therefore, reasonably assume that η is close to unity. Comparing the similar PL intensities of the boron BE and of the isoelectronic trap, we estimate a maximum trap concentration of about 10^{11} cm^{-3}. Similarly low concentrations were estimated for other isoelectronic traps such as the In-related trap in Si:In which is responsible for the *P,Q,R* luminescence lines,[8-11] or the trap generating the *A,B,C* lines.[7] Contrarily, the investigations of the Be-pair trap in silicon[19-21] have documented that if an isoelectronic trap is contained in the crystal to higher concentrations, for instance, up to 10^{16} cm^{-3} as for Be-Be, the luminescence is then correspondingly extraordinarily strong. The discrepancy between PL intensities and FeB-pair concentrations could therefore be an argument against the FeB luminescent trap model. However, the above reasoning implies that there is no essential competitive carrier recombination due to nonradiative recombination centers whose consideration would in turn weaken the point we are making.

A second problem is the fact that our Zeeman splittings are nearly isotropic and exhibit no indication of an axial nature of the PL trap. Taking for granted that the FeB pairs seen in DLTS and Hall-effect measurements are the same as those previously studied by Ludwig and Woodbury[41] in EPR, the FeB centers are highly anisotropic in contrast. These authors reported effective g values of $g'_{\parallel} = 2.068$ and $g'_{\perp} = 4.0$ for the EPR ground-state transition. The anisotropy is due to the large D term associated with the FeB-pair axis. Since the PL trap relatively strongly binds the extra particles in the excited state, we expect to also find anisotropic splittings in the excited state on a FeB-based model. We do not consider the principal possibility that a configuration change associated with an uncharged state which would be necessary to explain the $J=0$ ground-state momentum of the luminescent trap could result in more isotropic magnetic properties.

A third argument refers to the local-mode discrete sidebands observed energetically below the NP luminescence lines. The local-mode quantum energy, $\hbar\omega = 9.7$ meV, has been compared[12] to vibration energies of similar size observed in the photoluminescence from isoelectronic traps proposed to be associated with Cu ($\hbar\omega = 7.0$ meV), with Fe and In ($\hbar\omega = 9.2$ meV), Fe and Tl ($\hbar\omega = 5.4$ and 6.5 meV), and Cr and B ($\hbar\omega = 13.6$ meV). It was argued that when the optical centers are formed by pairs of these atoms alone, with the acceptors residing on substitutional sites and the transition ions residing on nearest, next-nearest, or third-nearest interstitial T_d sites, an analogy may exist with the well-authenticated cases of Li_iB_s, Li_iAl_s, and Li_iGa_s pairs.[50] These exhibit vibration energies close to 65 meV, nearly independent of the acceptor species and of isotopic substitution of the boron acceptor, but clearly shifting in energy upon isotopic Li substitution. In the latter cases, it was concluded[50] that the vibration of the interstitial Li is independent of the substitutional partner and that the interaction is entirely electrostatic in nature. If this were similar in the FeB luminescent trap we could regard the pair as a quasifree molecule and could not, in a simple manner, understand why unsymmetric E and T_2 vibrations could couple to the defect as earlier discussed in this paper; no indication exists in the spectra of a coupling to a totally symmetric A mode although the optical transition exciting this mode would be allowed. The coupling to E and T_2 modes would be rather suggestive of an additional cooperator in the defect enabling bending modes in the assumed purely electrostatic interaction model. Moreover, Schlesinger and McGill[51] also very recently generated the presently discussed PL spectrum in boron-doped silicon by iron diffusion and they showed that there is no isotopic shift in the NP line FeB_1^0 or in the phonon replicas FeB_1^1 and FeB_0^1 between ^{54}Fe- and ^{56}Fe-diffused samples.[52] They concluded that this is inconsistent with the identification of the phonon mode as a local vibration mode of iron as was suggested by Sauer and Weber.[12]

In conclusion, we have described the luminescent properties of a new isoelectronic trap in silicon. An optical level scheme of the center was derived. The formation conditions suggest that the center is associated with boron and iron atoms. Based on the present experimental data we cannot fully identify the trap, but we can show that an identification with FeB pairs is inconsistent with essential experimental observations.

ACKNOWLEDGMENTS

It is a pleasure to thank our colleagues H. Conzelmann for valuable discussions and K. Thonke for his assistance in the numerical solutions of various Zeeman secular matrices. J. Wagner [Max-Planck-Institut für Festkörperforschung (MPIF), Stuttgart] has kindly contributed the photoluminescence excitation spectra. We also thank K. Wünstel (MPIF) and P. Wagner (MPIF, now with Wacker Heliotronic, Burghausen) for the exchange of appropriately prepared samples and for many discussions of their DLTS data. This paper was supported by the Bundesministerium für Forschung und Technologie (BMFT) under Contract No. NT-2617.

[1]For reviews, see P. J. Dean, J. Lumin. 7, 51 (1973) (experimental); A. Baldereschi, J. Lumin. 7, 79 (1973) (theoretical); P. J. Dean and D. C. Herbert, in *Excitons,* Vol. 14 of *Topics in Current Physics,* edited by K. Cho (Springer, New York, 1979), p. 55.

[2]D. G. Thomas and J. J. Hopfield, Phys. Rev. 150, 680 (1966).

[3]F. A. Trumbore, M. Gerhenzon, and D. G. Thomas, Appl. Phys. Lett. 9, 4 (1966).

[4]T. N. Morgan, B. Welber, and R. N. Barghava, Phys. Rev. 166, 751 (1968).

[5]C. H. Henry, P. J. Dean, and J. D. Cuthbert, Phys. Rev. 166, 754 (1968).

[6]P. J. Dean, Phys. Rev. B 4, 2596 (1971).

[7]J. Weber, W. Schmid, and R. Sauer, J. Lumin. 18/19, 93 (1979); Phys. Rev. B 21, 2401 (1980).

[8]M. A. Vouk and E. C. Lightowlers, J. Lumin. 15, 357 (1977).

[9]G. S. Mitchard, S. A. Lyon, K. R. Elliott, and T. C. McGill, Solid State Commun. 29, 425 (1979).

[10]J. Weber, R. Sauer, and P. Wagner, J. Lumin. 24/25, 155 (1981).

[11]M. L. W. Thewalt, U. O. Ziemelis, and R. R. Parsons, Solid State Commun. 39, 27 (1981).

[12]R. Sauer and J. Weber, Physica 116B, 195 (1983).

[13]T. E. Schlesinger and T. C. McGill, Phys. Rev. B 25, 7850 (1982).

[14]T. E. Schlesinger, R. J. Hauenstein, R. M. Feenstra, and T. C. McGill, Solid State Commun. 46, 321 (1983).

[15]M. L. W. Thewalt, U. O. Ziemelis, S. P. Watkins, and R. R. Parsons, Can. J. Phys. 60, 1691 (1982).

[16]J. Weber, H. Bauch, and R. Sauer, Phys. Rev. B 25, 7688 (1982).

[17]S. P. Watkins, U. O. Ziemelis, M. L. W. Thewalt, and R. R. Parsons, Solid State Commun. 43, 687 (1982).

[18]J. A. Rostworowski and R. R. Parsons, Can. J. Phys. 59, 496 (1981), and references therein.

[19]M. O. Henry, E. C. Lightowlers, N. Killoran, D. J. Dunstan, and B. C. Cavenett, J. Phys. C 14, L255 (1981).

[20]N. Killoran, D. J. Dunstan, M. O. Henry, E. C. Lightowlers, and B. C. Cavenett, J. Phys. C 15, 6067 (1982).

[21]M. L. W. Thewalt, S. P. Watkins, U. O. Ziemelis, E. C. Lightowlers, and M. O. Henry, Solid State Commun. 44, 573 (1982).

[22]J. J. Hopfield, D. G. Thomas, and R. T. Lynch, Phys. Rev. Lett. 17, 312 (1966).

[23]H. Eisele, H. J. Paus, and J. Wagner, IEEE J. Quantum Electron. QE-18, 152 (1982).

[24]J. Wagner and R. Sauer, Phys. Rev. B 26, 3502 (1982), and references therein.

[25]R. Sauer, W. Schmid, and J. Weber, Solid State Commun. 27, 705 (1978).

[26]K. R. Elliott, S. A. Lyon, D. L. Smith, and T. C. McGill, Phys. Lett. 70A, 52 (1979).

[27]H. P. Gislason, B. Monemar, P. O. Holtz, P. J. Dean, and D. C. Herbert, J. Phys. C 15, 5467 (1982).

[28]J. v. W. Morgan and T. N. Morgan, Phys. Rev. B 1, 739 (1970).

[29]J. L. Merz, R. A. Faulkner, and P. J. Dean, Phys. Rev. 188, 1228 (1969).

[30]P. J. Dean and R. A. Faulkner, Phys. Rev. 185, 1064 (1969).

[31]J. Weber and P. Wagner, J. Phys. Soc. Jpn. 49A, 263 (1980).

[32]N. S. Minaev, A. V. Mudryi, and V. D. Tkachev, Fiz. Tekh. Poluprovdn. 13, 395 (1979) [Sov. Phys.—Semicond. 13, 233 (1979)].

[33]Y. H. Lee, R. L. Kleinhenz, and J. W. Corbett, Appl. Phys. Lett. 31, 142 (1977).

[34]H. J. Rijks, J. Bloem, and L. J. Giling, J. Appl. Phys. 50, 1370 (1979).

[35]E. Weber and H. G. Riotte, J. Appl. Phys. 51, 1484 (1980).

[36]K. L. Brower, Phys. Rev. B 14, 872 (1976).

[37]J. D. Struthers, J. Appl. Phys. 27, 1560 (1956).

[38]F. A. Trumbore, Bell Syst. Tech. J. 39, 205 (1960).

[39]C. B. Collins and R. O. Carlson, Phys. Rev. 108, 1409 (1957).

[40]H. H. Woodbury and G. W. Ludwig, Phys. Rev. 117, 102 (1960).

[41]G. W. Ludwig and H. H. Woodbury, in *Solid State Physics,* edited by F. Seitz and D. Turnbull (Academic, New York, 1962), Vol. 13.

[42]W. H. Shepherd and J. A. Turner, J. Phys. Chem. Solids 23, 1697 (1962).

[43]N. T. Bendik, V. S. Gornyk, and L. S. Milevskii, Fiz. Tverd. Tela (Leningrad) 12, 1340 (1970) [Sov. Phys.—Solid State 12, 1693 (1970)].

[44]H. Feichtinger, Acta Phys. Austriaca 51, 161 (1979).

[45]K. Graff and H. Pieper, J. Electrochem. Soc. 128, 669 (1981).

[46]K. Graff and H. Pieper, in *Semiconductor Silicon,* edited by H. R. Huff, R. J. Kriegler, and Y. Takeishi (The Electrochemical Society, Pennington, New Jersey, 1981), p. 331.

[47]K. Wünstel and P. Wagner, Appl. Phys. A 27, 207 (1982).

[48]L. C. Kimerling and J. L. Benton, Physica 116B, 297 (1983).

[49]W. Schmid, Phys. Status Solidi B 84, 529 (1977).

[50]R. C. Newman, *Infrared Studies of Crystal Defects* (Taylor and Francis, London, 1973).

[51]T. E. Schlesinger and T. C. McGill, Phys. Rev. B 28, 3643 (1983).

[52]These data conform with our unpublished experimental data on Fe isotope shifts.